

Original Article

Inorganic phosphate-osteogenic induction medium promotes osteogenic differentiation of valvular interstitial cells via the BMP-2/Smad1/5/9 and RhoA/ROCK-1 signaling pathways

Chao Lu^{1*}, Xiao Dong^{1*}, Wen Peng Yu¹, Jing Li Ding², Wei Yang¹, Yi Gong¹, Ji Chun Liu¹, Yan Hua Tang¹, Jian Jun Xu¹, Jian Liang Zhou¹

¹Department of Cardiovascular Surgery, The Second Affiliated Hospital of Nanchang University, Nanchang, China; ²Department of Gastroenterology, The Second Affiliated Hospital of Nanchang University, Nanchang, China. *Equal contributors.

Received November 22, 2019; Accepted June 9, 2020; Epub July 15, 2020; Published July 30, 2020

Abstract: Calcific aortic valve disease (CAVD) currently lacks a highly effective *in vitro* model. The presence of high concentrations of serum inorganic phosphate in patients with end-stage renal disease leads to calcification of vascular and aortic valves. Therefore, we applied inorganic phosphate to induce the osteogenic differentiation of valvular interstitial cells (VICs) and mimic its *in vivo* pathophysiological effects. Calcification and inflammatory response assays determined that inorganic phosphate-osteogenic induction medium (IP-OIM) was more efficient than classic osteogenic induction medium (OIM) containing organic glycerophosphate. Levels of BMP-2, RhoA, and ROCK-1 were significantly increased in IP-OIM cells. Knockdown efficiency of BMP-2- and RhoA-siRNA in VICs was evaluated, and expression of RhoA and its downstream target ROCK-1 was decreased after BMP-2-siRNA transfection. Moreover, ROCK-1 was significantly downregulated after RhoA knockdown, whereas expression of BMP-2 was unchanged. Interference of BMP-2 had a stronger anti-calcification effect than RhoA, further identifying BMP-2 as an upstream regulator of RhoA/ROCK-1. Stimulation of VICs by IP-OIM led to increased Smad1/5/9 phosphorylation, which peaked at 60 min, while pre-treatment of VICs with the Smad1/5/9 inhibitor Compound C attenuated VICs calcification. These results suggest that IP-OIM induced VICs osteogenic differentiation via Smad1/5/9 signaling. Knockdown of BMP-2 or RhoA also decreased Smad1/5/9 phosphorylation also decreased. We conclude that the RhoA/ROCK-1 axis participates in VICs osteogenic differentiation as a “bypass mediator” of the BMP-2/Smad1/5/9 signaling pathway.

Keywords: Valvular interstitial cells, calcified aortic valve disease, osteogenic differentiation, RhoA/ROCK-1, BMP-2, Smad

Introduction

Calcified aortic valve disease (CAVD) refers to the loss of valve elasticity due to valvular degeneration or calcium salt deposition that results in varying degrees of left ventricular outflow tract stenosis [1]. In some countries, CAVD is now the third most common cardiovascular disease, following hypertension and coronary heart disease, with an approximate incidence of 2.8% in patients over the age of 75 years that increases gradually with age [2]. However, CAVD pathogenesis has not been clearly described, and its treatment is mainly

surgical [3]. Further characterizing CAVD and improving the diversity of treatment options is of great importance, but the lack of relevant *in vitro* calcification models further limits advances in this area.

Valvular interstitial cells (VICs) act as a scaffold to maintain aortic valve leaflet morphology [4]. Previous studies have shown that, in addition to differentiating into normal fibroblasts, VICs can also display osteogenic phenotypes when stimulated under certain conditions. VICs are the main cell type that participate in aortic valve calcification [5], and exhibit the bone-tissue-

Stimulated osteogenesis of VICs via RhoA/ROCK-1 and BMP-2/Smad signaling

like characteristics that contribute to CAVD pathogenesis [6].

During osteogenic differentiation of bone mesenchymal stem cells (MSCs), high levels of bone morphogenetic protein-2 (BMP-2) can directly induce phosphorylation of the signal transducers Smad-1/5/9, whose nuclear translocation then promotes bone tissue differentiation and fracture healing [7]. Similarly, increasing the expression of RhoA (GTPase) and ROCK-1 (protein kinase) can also lead to osteogenic differentiation of MSCs [8]. BMP-2/Smad-1/5/9 and RhoA/ROCK-1 are the major signaling pathways involved in osteogenic differentiation [9, 10].

The current *in vitro* calcification model is established using classical osteogenic induction medium (OIM), which usually contains the organic phosphate glycerophosphate, but has some specific disadvantages, such as long modeling time (14-21 days) and low efficiency [11-13]. Previous studies have demonstrated that high levels of serum inorganic phosphate in patients with chronic kidney disease (CKD) often cause vascular calcification [14, 15]. Therefore, we hypothesized that directly using OIM containing inorganic phosphate (IP-OIM), which resembles *in vivo* calcification formation, has a more efficient osteogenic potential than OIM with organic phosphate (OIM).

In this study, we used IP-OIM and OIM to stimulate rat VICs and evaluated their osteogenic activity to determine whether inorganic phosphate exhibits higher efficiency than organic phosphate. Furthermore, we examined whether IP-OIM promoted osteogenic differentiation of VICs through the BMP-2/Smad1/5/9 and RhoA/ROCK-1 signaling pathways and explored whether these two pathways participate in VICs osteogenic differentiation.

Materials and methods

Reagents and solutions

Dulbecco's modified Eagle medium (DMEM, containing 4.5 g/L D-glucose, 25 mM HEPES), reduced serum medium (OPTI-MEM), fetal bovine serum (FBS), trypsin-EDTA, penicillin-streptomycin, and phosphate buffer saline (PBS) were purchased from Gibco (Grand Island, NY, USA). Type II collagenase and Triton

X-100 were purchased from Sigma-Aldrich (St. Louis, MO, USA). L-Ascorbic acid, β -glycerol-phosphate, dexamethasone, sodium dihydrogen phosphate, bovine serum albumin (BSA), Alizarin Red S, and Hanks' balanced salt solution (HBSS) were purchased from Sangon Biotech (Shanghai, China). Lipofectamine™ 3000 Transfection Reagent was purchased from Invitrogen (Carlsbad, CA, USA). The RNeasy Mini Kit was purchased from QIAGEN (Duesseldorf, Germany). The PrimeScript RT Master Mix and the TB Green Premix Ex Taq were purchased from Takara (Tokyo, Japan).

VICs isolation and culture

Male SD rats (8 weeks old) were purchased from the Sippr bk Laboratory Animals, Ltd. (Shanghai, China). All experimental protocols were approved by the Institutional Ethics Committee (NanChang University, SYXK2015-0001). Rats were fixed on the operating table following anesthesia, and 75% alcohol was used to disinfect the chest and abdomen. The heart was quickly removed and placed into 4°C pre-cooled PBS with 10% penicillin-streptomycin to avoid washed blood contamination. The tip of the heart was cut, and the heart tissues were cut along the left ventricular outflow tract to fully expose the aortic valve. The ventricular side of the aortic valve was then scraped lightly with the blunt end of a scalpel to remove endothelial cells. The distal one-third of the aortic leaflets was microdissected from the heart with microscissors, placed in HBSS containing 2 mg/ml type II collagenase, and digested for 2 h (37°C, 5% CO₂). After digestion, the cells were transferred into complete medium (DMEM, 20% FBS, 1% penicillin-streptomycin) and cultured in a humidified incubator (37°C, 5% CO₂). At 70%-80% confluence, the cells were diluted 1:3 using 0.25% trypsin-EDTA and then cultured with complete medium. Cells from passages three to five were used for further experiments.

Immunofluorescence assay

Logarithmic-phase cells were transferred to coverslips and allowed to attach. After 24 h, the complete medium was removed, and the cells were fixed with 4% paraformaldehyde for 20-30 min. The fixed cells were permeabilized by 0.5% Triton X-100 (5 min) and blocked in BSA for 30 min. The samples were incubated

Stimulated osteogenesis of VICs via RhoA/ROCK-1 and BMP-2/Smad signaling

Table 1. Primer sequences used in this research

Gene	Forward sequence (5'-3')	Reverse sequence (5'-3')
<i>GAPDH</i>	GACATGCCGCCTGGAGAAAC	AGCCCAGGATGCCCTTTAGT
<i>β-Actin</i>	TGTCACCAACTGGGACGATA	GGGGTGTGAAGGTCTCAA
<i>BMP-2</i>	CAGCGGAAGCGTCTTAAGTCCAG	GGCATGGTTGGTGGAGTTCAGG
<i>RhoA</i>	GCTTGTGGTAAGACATGCTTGCTC	GGCCTCAGACGGTCATAATCTTCC
<i>Rock-1</i>	ACCAGAAGGAGCTGAATGACATGC	GCACGCAACTGCTCAATATCACTC
<i>OST</i>	GACGATGATGACGACGACGATGAC	GTGTGCTGGCAGTGAAGGACTC
<i>ALP</i>	CACGGCGTCCATGAGCAGAAC	CAGGCACAGTGGTCAAGGTTGG
<i>Runx-2</i>	AACAGCAGCAGCAGCAGCAG	GCACGGAGCACAGGAAGTTGG

(4°C overnight) with anti-alpha smooth muscle actin (α -SMA) antibody (1:100, ab5694, Abcam, Cambridge, MA, USA) and anti-vimentin antibody (1:250, ab92547, Abcam) and subsequently incubated at room temperature for 2 h with goat anti-rabbit IgG H&L (1:200, ab1500-81, Abcam). Finally, DAPI (Solarbio, Beijing, China) was used to stain the cell nuclei. The cells were visualized by a fluorescence microscope (Nikon, Tokyo, Japan), and the relevant images were captured.

Model of VICs osteogenic differentiation

VICs osteogenic differentiation cultures: IP-OIM (sodium dihydrogen phosphate 10 mmol/l, L-Ascorbic acid 10 μ g/ml, dexamethasone 10 nmol/l add into complete medium) and OIM (β -glycerol-phosphate 10 mmol/l, L-Ascorbic acid 10 μ g/ml, dexamethasone 10 nmol/l add into complete medium) were used to culture VICs and promote their osteogenic differentiation. VICs cultured in complete medium set as control group (CON).

Western blot: Proteins were extracted following culture for 1 week using the M-PER Mammalian Protein Extraction Reagent (Thermo Fisher Scientific, Waltham, MA, USA), and their concentration was measured by the BCA method. Western blotting was performed to detect expression of BMP-2, RhoA, and ROCK-1. Briefly, 20 μ l of each protein sample was separated by electrophoresis (Bio-Rad, Hercules, CA, USA) and transferred to PVDF membranes (Pall Corporation, New York, USA). Subsequently, 5% BSA was used to block the membranes for 2 h, and the membranes were incubated overnight with anti-BMP-2 (1:500, ab14933, Abcam), anti-RhoA (1:250, ab54835, Abcam), and anti-ROCK-1 (1:500, ab97592, Abcam) antibodies in the presence of 4% BSA. The next day, the

membranes were washed three times with TBST and incubated with secondary antibodies for 2 h at room temperature. Finally, the membrane was incubated for 1 min in ECL Developer (Thermo, Berlin, Germany) and exposed with a TANON imager (Shanghai, China).

RNA isolation and quantitative PCR analysis:

An RNeasy mini kit was used for total RNA extraction following cell culture for 1 week. The RNA was reverse transcribed with the EASTWIN system (Suzhou, China). The expression levels of six calcification genes, namely RUNX-2, BMP-2, OST, RhoA, ROCK-1, and ALP were detected by real-time quantitative (RT-q) PCR using the StepOne real-time PCR system (Applied Biosystems, California, USA) with GAPDH as the internal reference gene. The $2^{-\Delta\Delta CT}$ method was employed to calculate the relative expression levels of the target genes for each sample compared to that of GAPDH. The PCR primers used are listed in **Table 1** (Sangon Biotech).

ALP activity assay and staining: Early-stage (6 days) osteogenic differentiation of VICs was evaluated using the BCIP/NBT ALP staining kit (Beyotime, Shanghai, China) according to the manufacturer's protocol. The activity of ALP was directly measured using the ALP activity detection kit (Solarbio).

Determination of calcium content and Alizarin Red staining:

The levels of late-stage osteogenic differentiation following 9 days of cell culture were observed by Alizarin Red staining as follows. The medium was removed and cells were fixed in 4% paraformaldehyde for 10 min and rinsed with 95% ethanol for 10 min. Then, 1% Alizarin Red was used to stain the cells, which were rinsed with 95% ethanol and scanned. The total protein relative calcium content was directly determined using a calcium content detection kit (MingDian, Shanghai, China).

Expression of inflammation-associated factors:

To determine the role of inflammatory NF- κ B pathway in osteogenic differentiation, the phosphorylation levels of NF- κ B were evaluated by Western blot after VICs were stimulated by IP-OIM or OIM for 120 min. The NF- κ B and

Stimulated osteogenesis of VICs via RhoA/ROCK-1 and BMP-2/Smad signaling

Table 2. siRNA sequence used in this research

siRNA	Sence (5'-3')	Atinsence (5'-3')
RhoA-siRNA1	CCAGUUCCCAGAGUUUUAUTT	AUAAACCUCUGGGAACUGGTT
RhoA-siRNA2	GCAGGUAGAGUUGGCUUUUATT	UAAAGCCAACUCUACCUGCTT
RhoA-siRNA3	UCAAGCAUUUCUGUCCAATT	UUUGGACAGAAUUGCUUGATT
BMP-2-siRNA1	CCCAGCGCUUCUUCUUAATT	UUGAAGAAGAAGCGUCGGTT
BMP-2-siRNA2	CCACGACGGUAAAGGACAUTT	AUGUCCUUUACCGUCGUGGTT
BMP-2-siRNA3	UCUGGUAAACUCUGUGAAUTT	AUUCACAGAGUUUACCAGATT

p-NF- κ B antibodies were purchased from Cell Signaling Technology (Danvers, MA, USA). On the 9th day of culture, the concentrations of inflammatory factors IL-6 and IL-8 in cell culture supernatants were analyzed using ELISA (Solarbio) according to the manufacturer's protocol.

siRNA silencing of BMP-2 and RhoA expression

Transfection efficiency assessment: According to the manufacturer's protocol, 1.5 μ l Lipofectamine™ 3000 and 15 pmol FAM-siRNA (Sangon Biotech) were diluted in OPTI-MEM and added to the culture medium to transfect VICs for 16-24 h. The culture medium was then removed, and the cell nuclei were stained by DAPI and observed using a fluorescence microscope.

Gene silencing efficiency assessment: We designed three siRNAs to interfere with RhoA and BMP-2 expression in VICs respectively. At the same time, β -actin-siRNA (PC, positive control) and NC-siRNA (NC, negative control) also used to transfect VICs respectively. Following transfection and culture with osteogenic induction media, RT-PCR and Western blotting were used to detect mRNA and protein expression levels of RhoA, ROCK-1, BMP-2 and β -actin. Based on these data, the siRNA with the highest knockdown efficiency was selected for subsequent experiments. The siRNA sequences are listed in **Table 2** (Sangon Biotech).

Osteogenic differentiation of VICs following transfection: The siRNA with the highest interference efficiency was used to transfect VICs. The cells were cultured with osteogenic induction media, and the ability of the siRNA to inhibit osteogenic differentiation was assessed by measuring the mRNA and protein expression levels of RUNX-2, BMP-2, OST, RhoA, ROCK-1,

and ALP. The evaluation of early- and late-stage osteogenic differentiation were also performed as described above.

Mechanism of VICs osteogenic differentiation

Role of Smad1/5/9 signaling pathway in VICs osteogenic differentiation:

VICs were cultured with osteogenic induction for 0, 15, 30, 60, and 120 min. The phosphorylation levels of Smad1/5/9 were assessed by Western blot, and the time period required for the highest phosphorylation level was determined. Subsequently, three working doses of the Smad1/5/9-specific inhibitor Compound C (MCE, New Jersey, USA) were added into the complete medium, and the VICs were pre-treated with these for 1 day. Then, the VICs were cultured with osteogenic induction, and Smad1/5/9 inhibitory efficiency was measured by Western blot. The working dose with the highest inhibitory efficiency was added to the osteogenic medium. The evaluation of early- and late-stage osteogenic differentiation were also performed as described above. The Smad1/5/9 Antibody Sampler Kit was purchased from Cell Signaling Technology.

Association between BMP-2-Smad1/5/9 and RhoA/ROCK-1 signaling:

VICs transfected with BMP-2-siRNA or RhoA-siRNA were cultured with osteogenic induction, and Western blotting was used to evaluate whether the low expression of BMP-2 or RhoA affected the phosphorylation level of Smad1/5/9.

Statistical analysis

Data were analyzed with Prism 7 (GraphPad Software, Inc., La Jolla, CA, USA) and presented as the mean \pm SD. Significant differences were identified using a one-way analysis of variance. A probability value of less than 0.05 ($P < 0.05$) was considered significant.

Results

Characterization of normal VICs

The cells isolated from rat aortic valves following digestion were visualized within 2 to 3 days by optical microscopy and exhibited round,

Stimulated osteogenesis of VICs via RhoA/ROCK-1 and BMP-2/Smad signaling

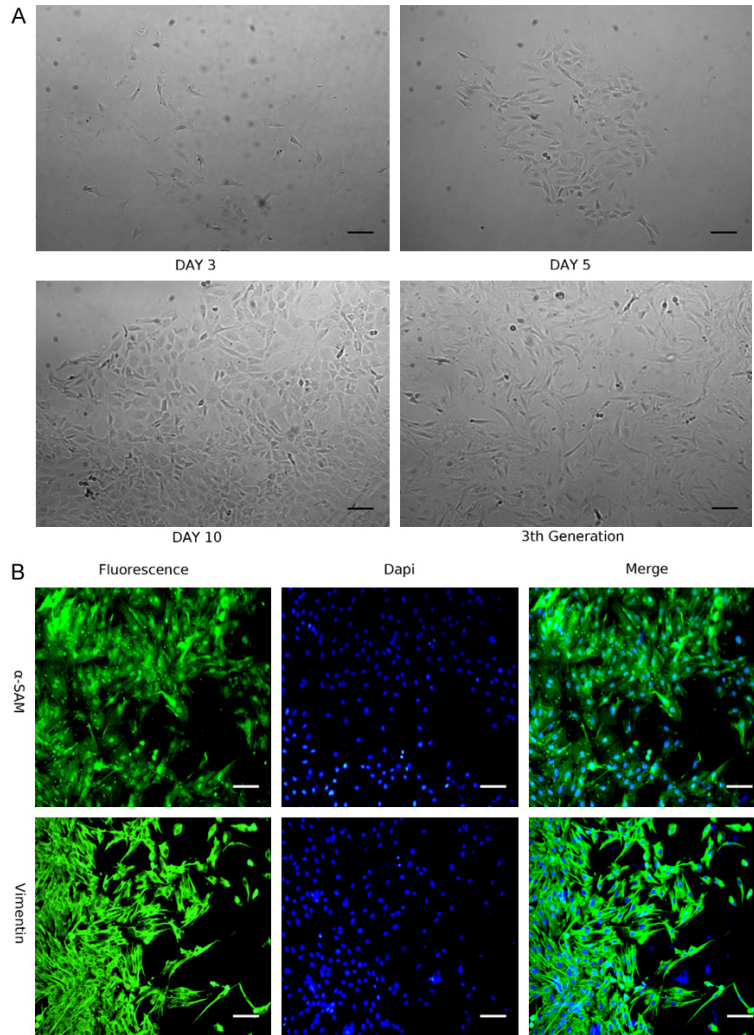


Figure 1. Microscopic observation of primary rat VICs following subculture. A. Optical microscopy shows spindle-shape cells; scale bar =20 μ m. B. Fluorescent staining of VICs markers α -SMA and vimentin. The expression rate of both proteins was over 90%; scale bar =20 μ m.

oval, or irregular shapes. Approximately 6 to 7 days later, the cells adopted a spindle-shape morphology (**Figure 1A**). The 4th generation of cells showed high homogeneity, and over 90% of the cells were stained positive for α -SMA and vimentin (**Figure 1B**), which are classical VICs-specific markers.

Model of VICs osteogenic differentiation

No significant change was noted in the cell morphology of the CON group at all time points. In contrast to the CON group, the IP-OIM group exhibited significant changes in cell phenotype on the 5th and 6th days. On the 6th day, the IP-OIM cells appeared to transform from a nor-

mal VICs phenotype to an irregular one, with a near absence of spindle-shaped cells by the 9th day. However, the cells in the OIM group did not show any phenotypic changes until the eighth and 9th days (**Figure 2**).

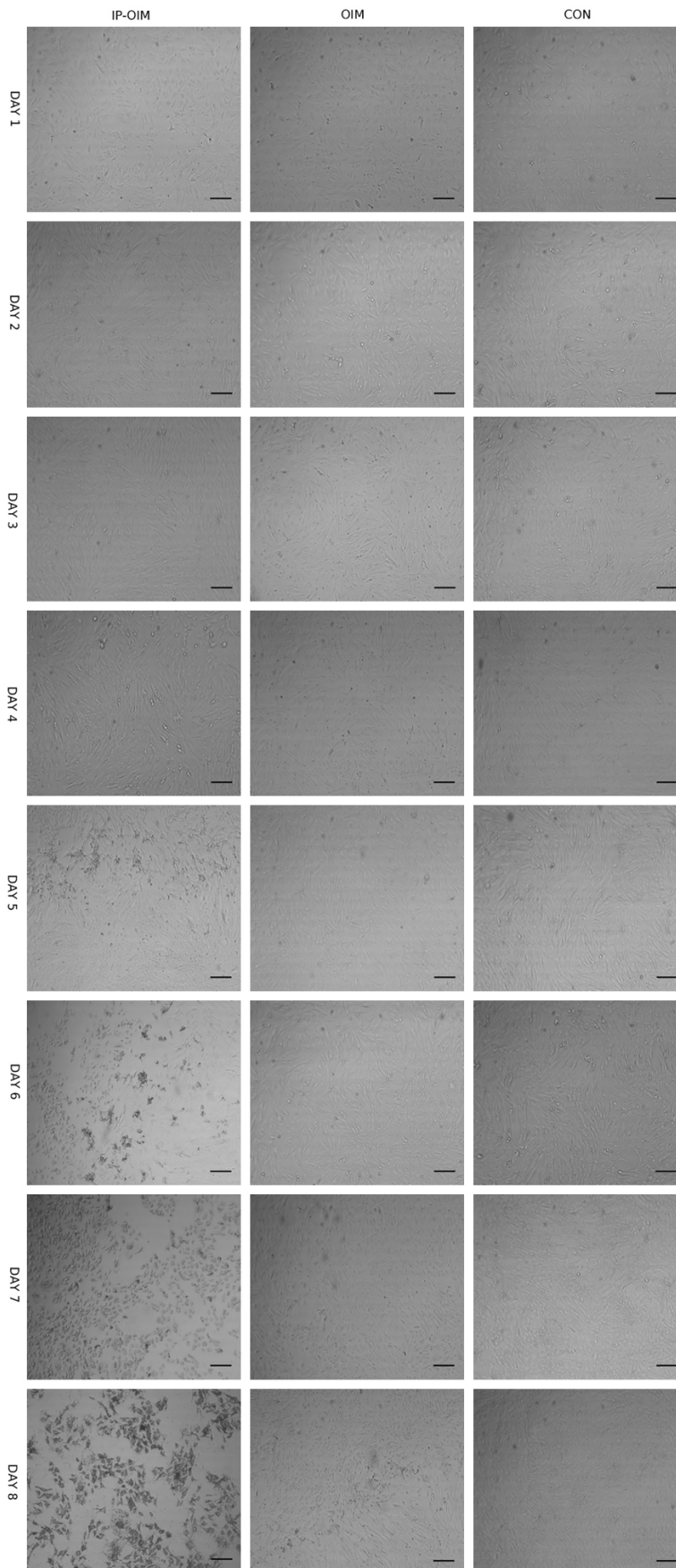
Western blotting of VICs (**Figure 3A**) showed the expression of BMP-2 in IP-OIM and OIM groups increased at varying degrees compared with the CON group ($P < 0.001$, $P < 0.05$), and levels of BMP-2 were higher in the IP-OIM group than in OIM cells ($P < 0.001$). We noted no significant difference in RhoA expression between the OIM and the CON groups, whereas RhoA expression in the IP-OIM group was significantly higher than in these two groups ($P < 0.001$ for both). Similarly, ROCK-1 levels were significantly higher in the IP-OIM group than in other groups ($P < 0.001$ for both), while the OIM cells exhibited no significant difference in ROCK-1 expression compared with the CON group.

Our RT-PCR analysis (**Figure 3B**) found that levels of BMP-2, RhoA, RUNX-2, ALP, and OST in the IP-OIM and OIM

groups were significantly higher than those of the CON group ($P < 0.001$ and $P < 0.05$, respectively), with their increased expression in the IP-OIM group notably significant ($P < 0.001$). Moreover, levels of ROCK-1 in the IP-OIM group were significantly higher than those of the OIM and CON groups ($P < 0.001$), although they did not significantly differ between the OIM and CON groups.

We determined that ALP activity (**Figure 3C**) in the IP-OIM (1.721 ± 0.101 U/mg) and OIM (0.84 ± 0.127 U/mg) groups was higher than that of the CON group (0.33 ± 0.09 U/mg) ($P < 0.001$ for both). We also noted significantly different ALP activity between the IP-OIM and

Stimulated osteogenesis of VICs via RhoA/ROCK-1 and BMP-2/Smad signaling



OIM groups ($P < 0.001$). ALP staining intensity was significantly different among the three groups (**Figure 3D**), a trend that was consistent with the results of the ALP activity assays. The calcium contents (**Figure 3E**) of the IP-OIM ($43.15 \pm 2.06 \mu\text{g}/\text{mg}$) and OIM ($19.69 \pm 1.24 \mu\text{g}/\text{mg}$) groups were higher than that of the CON group ($8.97 \pm 0.99 \mu\text{g}/\text{mg}$) ($P < 0.001$ for both), with the IP-OIM group calcium content highest of all ($P < 0.001$). Alizarin Red staining was significantly different (**Figure 3F**) in the three groups and corroborated the direct measurements of calcium within the cells.

Regarding the role of inflammation in osteogenic differentiation, NF- κ B phosphorylation was the highest in IP-OIM cells, although levels in both IP-OIM and OIM cells were higher than in the CON group ($P < 0.05$, **Figure 4A**). On the 9th day, the concentration of IL-8 in the IP-OIM ($171.95 \pm 15.38 \text{ pg}/\text{ml}$) and OIM ($92.27 \pm 8.99 \text{ pg}/\text{ml}$) groups was higher than that of the CON group ($48.18 \pm 10.92 \text{ pg}/\text{ml}$), again with IP-OIM cells showing significantly higher levels of IL-8 than OIM cells ($P < 0.001$, **Figure 4B**). Concentrations of IL-6 followed a similar pattern as IL-8: IP-OIM group ($492.59 \pm 16.96 \text{ pg}/\text{ml}$) > OIM group ($250.93 \pm 17.66 \text{ pg}/\text{ml}$) > CON group ($101.91 \pm 12.50 \text{ pg}/\text{ml}$) ($P < 0.001$, **Figure 4C**).

These data suggest that during early- and late-stage VICs osteogenic differentiation, IP-OIM led to higher efficiency than OIM and activated a stronger inflammatory response. Thus, in subsequent ex-

Stimulated osteogenesis of VICs via RhoA/ROCK-1 and BMP-2/Smad signaling



Figure 2. Changes in VICs morphology after growth in OIM, IP-OIM, and complete medium (CON). Cells were observed with optical microscopy at the designated timepoints; scale bar =50 μ m.

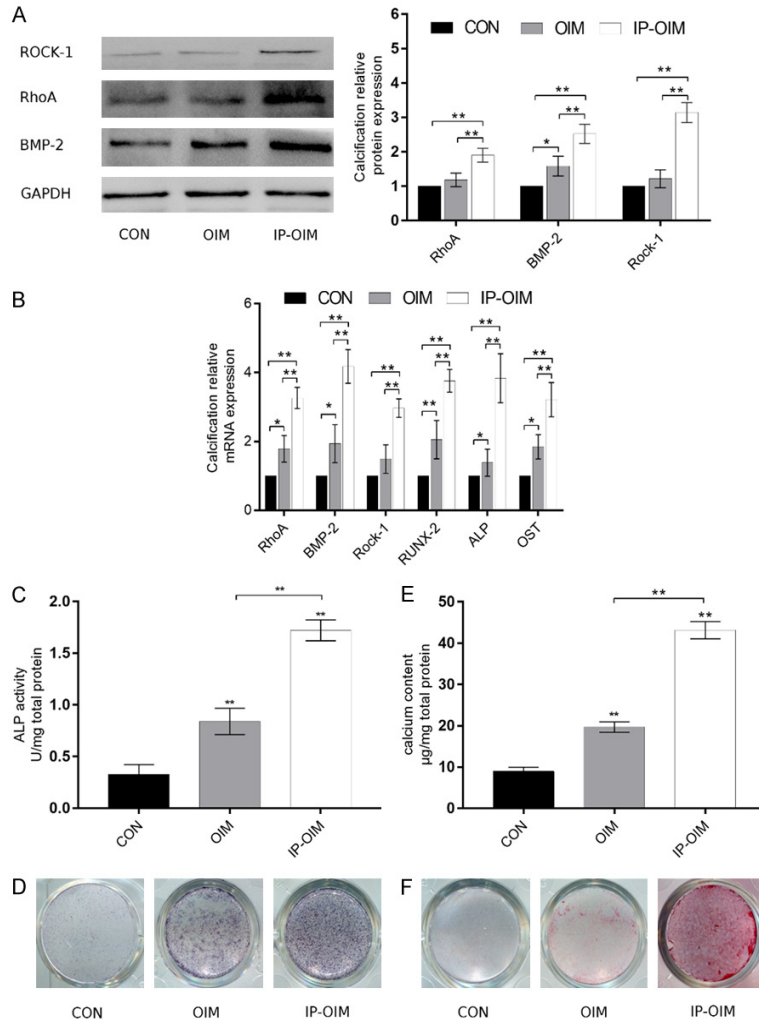


Figure 3. Expression of calcification-associated factors in VICs cultured in complete medium (CON), OIM, and IP-OIM. A. Western blots of cell proteins on the 7th day of culture (N=3; *P<0.05, **P<0.001). B. RT-PCR analysis of calcification factors BMP-2, RhoA, ROCK-1, RUNX-2, ALP, and OST on the 7th day of culture (N=3; *P<0.05, **P<0.001). C. ALP activity assays were performed on the 6th day (N=3; *P<0.05, **P<0.001). D. ALP staining on the 6th day. E. Measurement of calcium content on the 9th day (N=3; *P<0.05, **P<0.001). F. Alizarin Red staining on the 9th day.

periments, IP-OIM was used to stimulate VICs osteogenic differentiation.

siRNA silencing of BMP-2 and RhoA expression

We determined that siRNA transfection efficiency was approximately 80% via monitoring fluorescently tagged (FAM)-siRNA (**Figure 5A**). RT-PCR of cells after transfection with RhoA-siRNA (**Figure 5B**) showed the siRNA2 and siRNA3 groups caused a significant decrease in levels of RhoA compared with the CON group (P<0.001, P<0.05). Differences in RNA expression between the siRNA1 and siRNA2 groups were significant (P<0.001). Similarly, expression of ROCK-1, which encodes a downstream target of RhoA, was decreased in the siRNA2 and siRNA3 groups compared with the CON group (P<0.001, P<0.05), while siRNA1 did not cause a significant decrease in ROCK-1 expression. Levels of ROCK-1 significantly differed between the siRNA1 and siRNA2 groups (P<0.001). However, we noted no change in the expression of BMP-2 following RhoA silencing.

Based on our Western blot results of the target proteins (**Figure 5C**), the siRNA2 and siRNA3 groups caused significantly decreased RhoA expression compared with the CON group (P<0.001, P<0.05), while the siRNA1 group did not cause a significant decrease. The effects between the siRNA1 and the siRNA2 groups were significantly different (P<0.001). Consistent with RhoA expression patterns, levels of the downstream target ROCK-1 were partially decreased, whereas the expression of BMP-2 remained unchanged.

Following transfection of BMP-2-siRNA into VICs, our RT-PCR analysis (**Figure 5D**) indicated

Stimulated osteogenesis of VICs via RhoA/ROCK-1 and BMP-2/Smad signaling

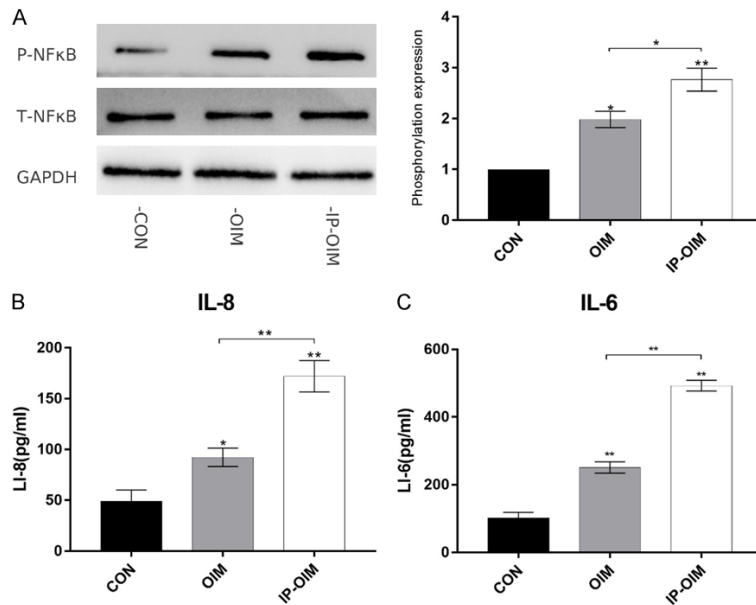


Figure 4. Induction of inflammatory responses in VICs following culture in IP-OIM, OIM, or complete medium. (A) After stimulation for 120 min, NF- κ B phosphorylation levels were assessed via Western blot (N=3; *P<0.05, **P<0.001). On the 7th day of culture, IL-8 (B) and IL-6 (C) concentrations in cell culture supernatants were determined by ELISA (N=3; *P<0.05, **P<0.001).

that expression of BMP-2 in the siRNA1 and siRNA2 groups decreased compared with that noted in the CON group (P<0.001, P<0.05), while the siRNA3 group did not cause a significant decrease in its expression. siRNA1 transfection exerted the greatest effect and was significantly different to that of the other two groups (P<0.05, P<0.001). Notably, expression levels of RhoA and ROCK-1 also decreased following silencing of BMP-2. Our Western blot analysis (**Figure 5E**) revealed similar results regarding BMP-2 expression as those obtained by RT-PCR: expression of BMP-2, RhoA, and ROCK-1 decreased to some extent, with the siRNA1 group exerting the strongest effect. In summary, we found that the RhoA-siRNA2 and BMP-2-siRNA1 groups exhibited the highest interference efficiency, so these two sequences were used in subsequent experiments. In addition, after silencing of BMP-2 in VICs, expression of both RhoA and its downstream target ROCK-1 were downregulated. However, silencing of RhoA only downregulated ROCK-1 expression, whereas BMP-2 levels were unchanged.

Anti-calcification effects of siRNA transfection

After transfection with BMP-2- and RhoA-siRNA respectively, VICs were cultured in IP-OIM, and

the expression of the calcification-associated factors BMP-2, RhoA, ROCK-1, ALP, RUNX-2, and OST was assessed by Western blot (**Figure 6A**). As noted previously, BMP-2 expression in the si-RhoA group was not significantly different than the CON group but was significantly decreased in the si-BMP-2 group (P<0.001). However, the expression levels of RhoA following si-RhoA and si-BMP-2 transfection were lower than those of the CON group (P<0.001 for both) but were not significantly different between the two siRNA groups. Expression levels of ROCK-1 were consistent with those of RhoA expression. Levels of the other calcification-related factors, such as ALP, were decreased in the si-RhoA group and si-BMP-2 group compared with

the CON group (P<0.001 for both), although ALP expression was significantly more decreased in the si-BMP-2 group than in the si-RhoA group (P<0.05). Changes in the expression of OST and RUNX-2 were similar to those of ALP, with the si-RhoA and si-BMP-2 groups exhibiting significantly lower levels of these factors than the CON group (P<0.05, P<0.001; P<0.05, P<0.001); the most significant difference was noted in the si-BMP-2 group (P<0.05; P<0.001). The mRNA expression of the calcification-related factors was also downregulated in the si-BMP-2 and si-RhoA groups compared with the CON group. However, there were some results differed from those noted in the Western blot analysis, as expression of RhoA in these two groups were significantly different from each other (P<0.05), but expression of OST did not change significantly between the si-RhoA and si-BMP-2 groups (**Figure 6B**).

ALP activity levels on the 6th day (**Figure 6C**) in the si-RhoA (1.154 ± 0.156 U/mg) and si-BMP-2 (0.565 ± 0.098 U/mg) groups were significantly decreased compared with those of the CON group (1.984 ± 0.204 U/mg) (P<0.001 for both), with the si-BMP-2 group showing the lowest levels of all groups (P<0.001). This same pattern was observed by ALP staining (**Figure 6D**),

Stimulated osteogenesis of VICs via RhoA/ROCK-1 and BMP-2/Smad signaling

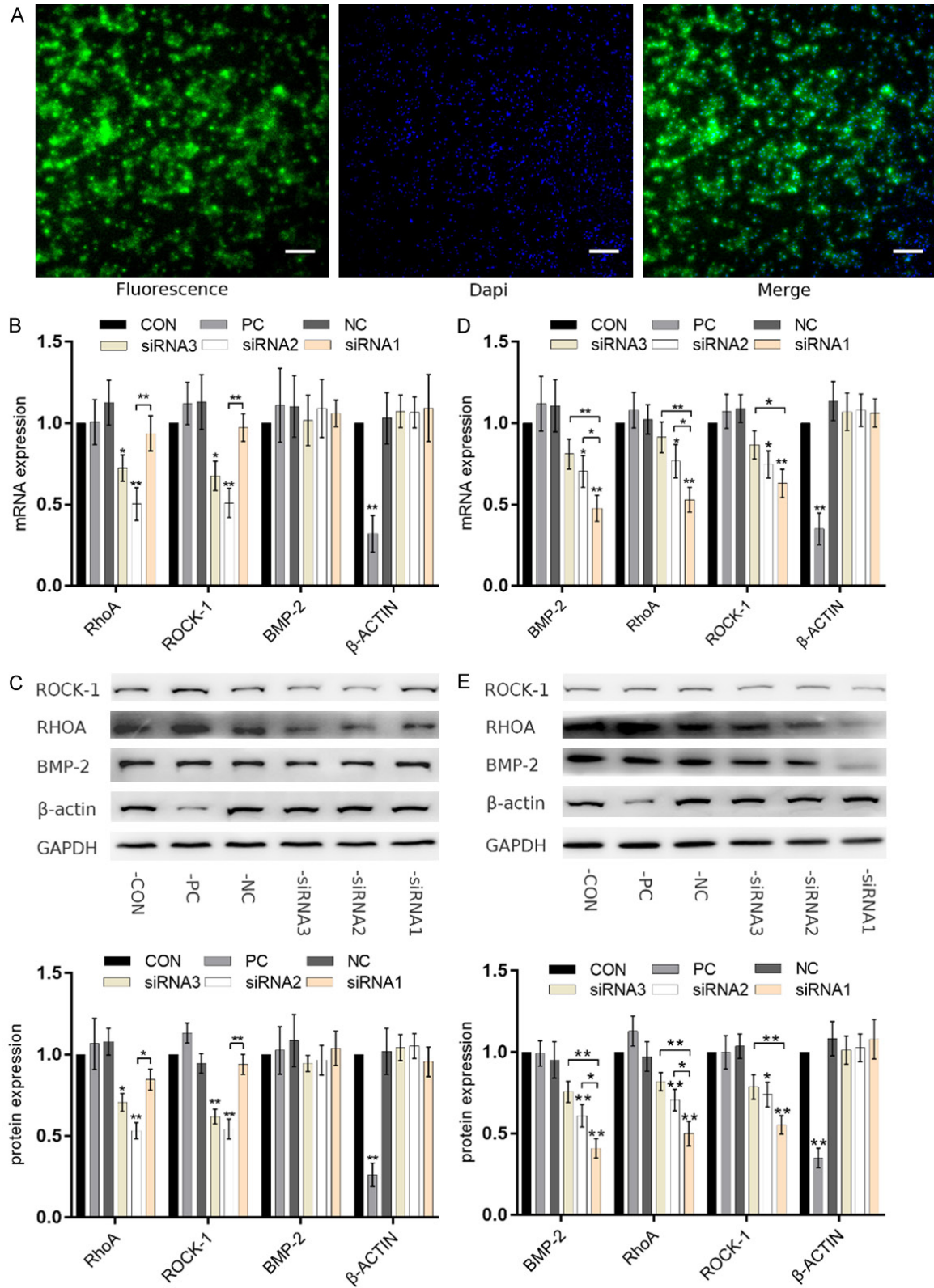


Figure 5. Assessment of siRNA transfection efficiency and target gene knockdown. A. Efficiency of fluorescently tagged FAM-siRNA transfection into VICs; scale bar =50 μm. B. RT-PCR of target genes following transfection of RhoA-siRNA (N=3; *P<0.05, **P<0.001). C. Western blot of target proteins following transfection of RhoA-siRNA (N=3; *P<0.05, **P<0.001). D. RT-PCR of target genes after transfection of BMP-2-siRNA (N=3; *P<0.05, **P<0.001). E. Western blot of target proteins after transfection of BMP-2-siRNA (N=3; *P<0.05, **P<0.001).

Stimulated osteogenesis of VICs via RhoA/ROCK-1 and BMP-2/Smad signaling

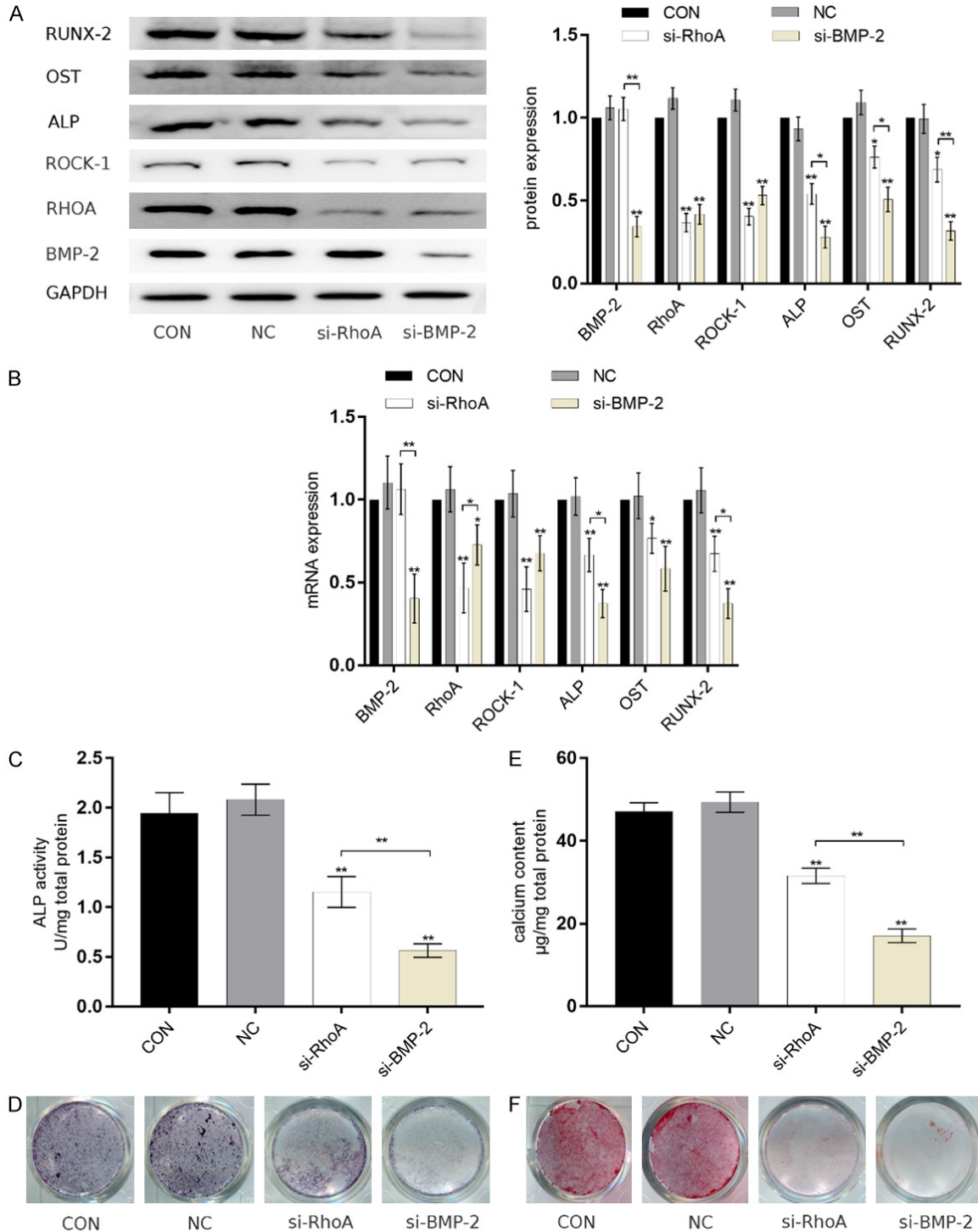


Figure 6. Expression of calcification factors following knockdown of BMP-2 and RhoA. **A.** Western blot following transfection of RhoA-siRNA2 and BMP-2-siRNA1 into VICs (N=3; *P< 0.05, **P<0.001). **B.** RT-PCR analysis of the same factors following transfection with RhoA-siRNA2 and BMP-2-siRNA1 (N=3; *P<0.05, **P<0.001). **C.** ALP activity assay on the 6th day (N=3; *P<0.05, ** P<0.001). **D.** ALP staining on the 6th day. **E.** Detection of calcium content on the 9th day (N=3; *P<0.05, **P<0.001). **F.** Alizarin red staining on the 9th day.

where si-BMP-2 exhibited the lowest color intensity. Calcium content on the ninth day

(**Figure 6E**) was significantly lower in the si-RhoA (31.58±1.869 µl/mg) and the si-BMP-2

Stimulated osteogenesis of VICs via RhoA/ROCK-1 and BMP-2/Smad signaling

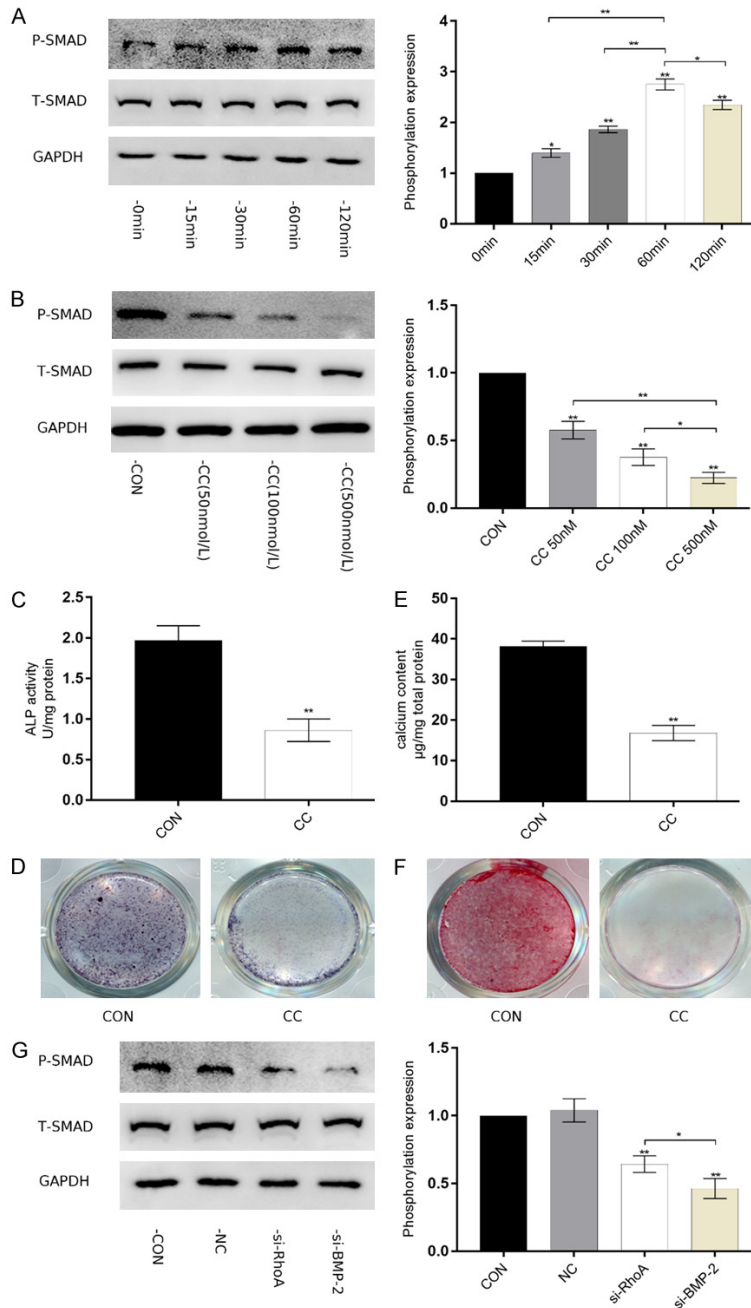


Figure 7. Phosphorylation of Smad1/5/9 during VICs osteogenic differentiation. A. Cells were stimulated with IP-OIM for 15, 30, 60, and 120 min to detect Smad1/5/9 phosphorylation levels. B. The inhibitory efficiency of the Smad1/5/9-specific inhibitor Compound C (CC) was determined by pre-treating VICs with varying concentrations of Compound C. C. ALP activity was measured on the 6th day of co-culture with Compound C (N=3; *P<0.05, **P<0.001). D. ALP staining was performed on the 6th day. E. Detection of calcium content on the 9th day of Compound C treatment (N=3; *P<0.05, **P<0.001). F. Alizarin Red staining of cells on the 9th day. G. Phosphorylation levels of Smad1/5/9 in siRNA-transfected VICs stimulated with IP-OIM for 60 min.

(17.08±1.664 µg/mg) groups compared with the CON group (47.14±2.104 µg/mg) (P<0.001

for both). The decrease in calcium content of the si-BMP-2 group was most notable of all the groups and was significantly lower than that of the si-RhoA group (P<0.001). The same pattern was observed after Alizarin Red staining (Figure 6F).

In summary, silencing of BMP-2 or RhoA led to the downregulation of calcification-related factors, namely ALP, OST, and RUNX-2, at the mRNA or protein level, with the most significant downregulation noted in the si-BMP-2 group. The ALP activity assays and ALP staining demonstrated that the silencing of BMP-2 and RhoA, particularly BMP-2, could negatively affect early-stage VICs osteogenic differentiation. Direct measurement of calcium content, together with Alizarin Red staining, indicated that downregulation of BMP-2 and RhoA could also impact late-stage VICs osteogenic differentiation, again with silencing of BMP-2 exerting the greatest effects. Transfection with si-BMP-2 downregulated RhoA and ROCK-1 expression, whereas interference of RhoA only decreased ROCK-1 expression.

Mechanism of VICs osteogenic differentiation

We used IP-OIM to stimulate VICs for different time periods and found that the phosphorylation of Smad1/5/9 were increased from 15 min of treatment (Figure 7A) and reached their highest peak at 60 min, suggesting that IP-OIM induced phosphorylation of Smad1/5/9 signaling path-

way. Subsequently, we pre-treated VICs with different concentrations of the Smad1/5/9

pathway-specific inhibitor Compound C and measured changes in phosphorylation after VICs stimulation with IP-OIM for 60 min. Compound C pre-treatment reduced the phosphorylation levels of Smad1/5/9, with the most potent effect noted at 500 nmol/l (**Figure 7B**). VICs were then co-cultured with 500 nmol/l Compound C and IP-OIM to assess whether inhibition of Smad1/5/9 reduced their osteogenic differentiation. On the 6th day Compound C (CC) group (0.862 ± 0.138 U/mg) exhibited significantly lower ALP levels than the CON group (1.965 ± 0.186 U/mg) ($P < 0.001$) (**Figure 7C**), which was confirmed by ALP staining (**Figure 7D**). Calcium content measured on the 9th day (**Figure 7E**) indicated that the CC group (16.82 ± 1.87 $\mu\text{g}/\text{mg}$) exhibited significantly lower levels of calcium than the CON group (38.18 ± 1.31 $\mu\text{g}/\text{mg}$) ($P < 0.001$), which was verified by Alizarin Red staining too (**Figure 7F**).

To verify the association between BMP-2/Smad1/5/9 and RhoA/ROCK-1 signaling in osteogenic differentiation, we used IP-OIM to stimulate VICs cells transfected with si-BMP-2 and si-RhoA for 60 min respectively. Smad1/5/9 phosphorylation levels in the si-RhoA and si-BMP-2 groups were significantly lower than those of the CON group (**Figure 7G**, $P < 0.001$ for both), with the si-BMP-2 group showing the most dramatic decrease of all groups ($P < 0.05$).

Discussion

The incidence of CAVD increases every year, in North America alone, 85,000 new cases have been identified and have led to 15,000 mortalities per year [16]. The number of CAVD patients is predicted to reach 4.5 million by 2030 [17], highlighting the importance of identifying potential therapies for this disease. Constructing an efficient and relevant model that reflects the *in vivo* pathological changes of CAVD will advance this research. Swetha et al. [18] showed that aortic valve calcification and vascular wall calcification in patients with end-stage kidney disease occurred mostly due to elevated serum inorganic phosphate caused by an imbalance of pyrophosphate (PPI) and inorganic phosphate (IP). *In vivo*, PPI can inhibit the deposition of phosphate and calcium, while IP or ALP can hydrolyze PPI to relieve this inhibition and promote calcification. Liu et al. [19] used serum from uremia patients

that contained high concentration of IP to successfully promote arterial smooth muscle cell osteogenic differentiation, thus confirming the effect of IP on osteogenic differentiation. Furthermore, studies by Neven and Yamada have shown that the use of PPI or other IP inhibitors can exert an anti-calcification effect [20, 21]. However, few parallel comparisons of IP-OIM and OIM efficiency have been performed. Here, we found that IP-OIM induced stronger early- and late-stage VICs osteogenic differentiation than OIM and caused notable calcium deposits following 9 days of treatment, while treatment with OIM required 14 or even 21 days [11-13]. Goto et al. [22] compared the effects of IP-OIM and OIM and reached similar conclusions to those of our study, but the mechanism of their action was not fully explored. Aredshiryajimi et al. [23] used IP-OIM to promote MSCs osteogenic differentiation and suggested that IP-OIM induces *in vitro* osteogenic differentiation similar to that which occurs *in vivo* and is considerably less toxic than OIM but is significantly less efficient than OIM; however, this finding may be related to the different types of cells used in that study. Inflammation also plays an important role in VICs osteogenic differentiation [24]. We found that IP-OIM more strongly promotes inflammation, induces greater NF- κ B phosphorylation, and leads to more IL-6 and IL-8 release than OIM. Notably, both IL-6 and IL-8 likely have a direct relationship with heart valve calcification [25, 26]. Specifically, the release of IL-6 by VICs promotes the osteogenic transition and mineralization of cells through the production of BMP-2 [27].

The BMP-2 is a regulatory protein member of the transforming growth factor beta (TGF- β) superfamily that induces osteoblast differentiation and bone formation by activating various downstream factors and promoting MSCs transformation to osteogenic phenotypes [28, 29]. Expression of BMP-2 is significantly upregulated during the osteogenic differentiation of several other cells and tissues, such as vascular smooth muscle cells and dental follicle stem cells [30, 31]. Calcification of the heart valve results from active transformation of VICs to the osteoblast-like cell phenotype, which involves the regulation of multiple osteogenic factors [32], including the positive role of BMP-2 [6, 33]. BMP-2 activates the Smad sig-

nal pathway, which is necessary for osteoblast activation and extracellular matrix calcification [34]. Specifically, BMP-2 mediates the phosphorylation of Smad1, Smad5, and Smad9 that then form a complex with their common partner Smad4, which translocates to the nucleus and directly regulates target gene expression. Smad4 and Smad binding elements can also indirectly regulate target gene expression by interacting with transcription factors, receptor co-activators, or nuclear receptor co-repressors [35], RUNX-2 is one target gene of the BMP-2/Smad1/5/9 signaling pathway [36, 37]. Following VICs stimulation, we found that IP-OIM led to higher levels of BMP-2 expression at both the mRNA and protein level, suggesting that IP-OIM demonstrates higher osteogenic efficiency than OIM. After silencing BMP-2, expression of the calcification-related factors RUNX-2, ALP, and OST showed varying degrees of downregulation. Our ALP and calcium activity and content assays indicate the anti-calcification effects of BMP-2 silencing occurred during both the early and late stages of osteogenesis. In addition, IP-OIM treatment increased the phosphorylation of Smad1/5/9, which peaked at 60 min, whereas interference with BMP-2 expression decreased phosphorylation levels. The Smad1/5/9 pathway inhibitor Compound C further reduced the osteogenic differentiation of VICs. Based on these results, we conclude that IP-OIM induces osteogenic differentiation of VICs via the BMP-2/Smad1/5/9 signaling pathway.

The RhoA/ROCK-1 axis is commonly activated in various types of tissues and cells and participates in many cellular processes, including growth, proliferation, apoptosis, differentiation, cytoskeleton regulation, adhesion, attachment, deformation, and movement. Previous studies have indicated that RhoA/ROCK-1 signaling plays an important regulatory role in neuron-like cell differentiation, osteogenic differentiation, cartilage differentiation, and epidermal cell differentiation of MSCs [38-41]. The protein expression levels of RhoA and ROCK-1 in VICs exhibited no significant increase following stimulation with OIM, and only mRNA levels of RhoA increased. In contrast, mRNA and protein expression of RhoA and ROCK-1 was significantly upregulated in VICs after stimulation with IP-OIM. During calcification cultures, the phenotype of cells in the CON group did not change,

whereas VICs in the IP-OIM group began exhibiting altered, irregular morphology on the 5th day that was nearly complete by the 9th day, while OIM did not cause significant changes in cell morphology until the 9th day. Gu et al. [42] determined that phenotypic changes of VICs were accompanied by activation of the RhoA/ROCK-1 signaling pathway. Farrar et al. [43] used a 3D tension model to verify that these phenotypic changes will activate RhoA, causing a subsequent distortion in the intracellular tension balance that leads to pre-osteogenesis stage. Therefore, IP-OIM can activate and induce expression of RhoA and its downstream target ROCK-1 by affecting the phenotype of the cells and causing more rapid VICs transformation than OIM. The calcification-related factors RUNX-2, ALP, and OST exhibited different degrees of downregulation after silencing of RhoA, and levels of calcium content significantly decreased after si-RhoA transfection, suggesting that interference of RhoA has an anti-calcification effect in the early and late stages of osteogenesis. Thus, we concluded that the RhoA/ROCK-1 axis is an important signaling pathway in the IP-OIM-induced osteogenic differentiation of VICs.

Following interference of BMP-2 expression, expression of both RhoA and ROCK-1 was downregulated, while RhoA interference affected only ROCK-1 expression. The anti-osteogenic effect of BMP-2 on VICs was stronger than that of RhoA interference, so we concluded that BMP-2 is an upstream regulator of RhoA and ROCK-1. To date, less reports on the association between BMP-2 and RhoA in the context of VICs osteogenic differentiation have been published. However, Wang et al. [44] demonstrated that the RhoA/ROCK-1 signaling pathway is involved in BMP-2 activation and Smad phosphorylation during MSCs osteogenic differentiation. Zhu et al. [45] indicated that RhoA/ROCK-1 expression promotes phosphorylation of Smad1/5/9 and its subsequent nuclear translocation by BMP-2 during the differentiation of human corneal endothelial cells into neural progenitor cells. Because silencing of RhoA, decreased levels of p-Smad1/5/9 in our study, but not stronger than silencing of BMP-2, we considered that RhoA/ROCK-1 signaling is involved in BMP-2/Smad1/5/9 phosphorylation, which subsequently upregulates the expression of other

Stimulated osteogenesis of VICs via RhoA/ROCK-1 and BMP-2/Smad signaling

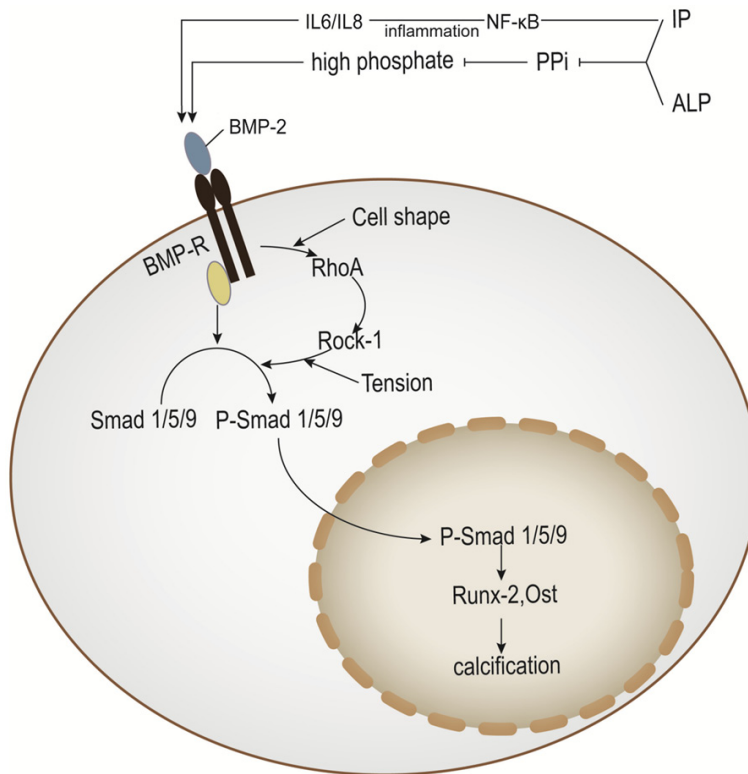


Figure 8. Proposed mechanism of IP-OIM-mediated stimulation of VICs osteogenic differentiation.

calcification-related factors. Gu et al. [42] found that RhoA/ROCK-1 did not directly cause osteogenic differentiation of VICs but activated osteogenic differentiation signaling by affecting the intracellular tension balance. Sung et al. [46] showed that RhoA/ROCK-1 is involved in the activation of osteogenic differentiation via induction of SOX-9 expression. In the current study, we determined that RhoA/ROCK-1 induced osteogenic differentiation in VICs through phosphorylation of Smad1/5/9.

Aortic stenosis caused by valve calcification was previously considered to be a degenerative change but has since been shown to be caused by various factors [47]. Specifically, lipid deposition, osteogenic differentiation, changes in cell phenotype, endothelial injury, and inflammatory mediators have been verified to promote aortic calcification [48-52]. Our research further demonstrates that during the calcification of VICs, osteogenic differentiation, inflammation, and altered cell phenotypes do not occur independently but are related through BMP-2/RhoA/ROCK-1/Smad signaling (**Figure 8**).

In conclusion, IP-OIM can induce stronger *in vitro* VICs osteogenic differentiation and inflammatory responses than OIM, indicating its value in future research involving CAVD. Mechanistically, during VICs osteogenic differentiation, IP-OIM promotes phosphorylation of Smad1/5/9 by direct upregulation of BMP-2, which leads to calcification. Besides, change in cell morphology leads to RhoA/ROCK-1 activation also contributes to Smad1/5/9 phosphorylation. BMP-2 is an upstream regulator of RhoA/ROCK-1, although the mechanism of this interaction requires further investigation.

Acknowledgements

This work was funded by the National High-Tech Research and Development Program (863 Program) of China (grant no. 2014AA020539), National Natural Science Foundation of China (grant nos. 81770388, 81860079, and 81660070), Outstanding Young Talent Program of Jiangxi Province (grant no. 20162BCB23059), National Science Foundation of Jiangxi Province (grant nos. 20151BAB205007, 20161BBI90015, and 20171ACB21061), and Research Project of Jiangxi Provincial Department of Education (grant no. 150274).

Disclosure of conflict of interest

None.

Address correspondence to: Jian Liang Zhou, Department of Cardiovascular Surgery, The Second Affiliated Hospital of Nanchang University, No. 1 Minde Road, Nanchang 330006, Jiangxi, China. Tel: +86-13767117511; E-mail: zhoujianliang2010@163.com

References

- [1] Lindman BR, Clavel MA, Mathieu P, Lung B, Lancellotti P, Otto CM and Pibarot P. Calcific aortic stenosis. *Nat Rev Dis Primers* 2016; 2: 16006.

Stimulated osteogenesis of VICs via RhoA/ROCK-1 and BMP-2/Smad signaling

- [2] Peltonen T, Ohukainen P, Ruskoaho H and Rysä J. Targeting vasoactive peptides for managing calcific aortic valve disease. *Ann Med* 2017; 1: 63-74.
- [3] Liskova J, Hadraba D, Filova E, Konarik M, Pirk J, Jelen K and Bacakova L. Valve interstitial cell culture: production of mature type I collagen and precise detection. *Microsc Res Tech* 2017; 8: 936-942.
- [4] Zhiduleva EV, Irtyuga OB, Shishkova AA, Ignat'eva EV, Kostina AS, Levchuk KA, Golovkin AS, Rylov AY, Kostareva AA, Moiseeva OM, Malashicheva AB and Gordeev ML. Cellular mechanisms of aortic valve calcification. *Bull Exp Biol Med* 2018; 3: 371-375.
- [5] Boström KI, Rajamannan NM and Towler DA. The regulation of valvular and vascular sclerosis by osteogenic morphogens. *Circ Res* 2011; 5: 564-577.
- [6] Mohler ER, Gannon F, Reynolds C, Zimmerman R, Keane MG and Kaplan FS. Bone formation and inflammation in cardiac valves. *Circulation* 2001; 11: 1522-1528.
- [7] Lo YC, Chang YH, Wei BL, Huang YL and Chiou WF. Betulinic acid stimulates the differentiation and mineralization of osteoblastic MC3T3-E1 cells: involvement of BMP/Runx2 and beta-catenin signals. *J Agric Food Chem* 2010; 11: 6643-6649.
- [8] Arnsdorf EJ, Tummala P, Kwon RY and Jacobs CR. Mechanically induced osteogenic differentiation—the role of RhoA, ROCKII and cytoskeletal dynamics. *J Cell Sci* 2009; 122: 546-553.
- [9] Zhang T, Lin S, Shao X, Shi S, Zhang Q, Xue C, Lin Y, Zhu B and Cai X. Regulating osteogenesis and adipogenesis in adipose-derived stem cells by controlling underlying substrate stiffness. *J Cell Physiol* 2018; 4: 3418-3428.
- [10] Kumar Y, Biswas T, Thacker G, Kanaujiya JK, Kumar S, Shukla A, Khan K, Sanyal S, Chattopadhyay N, Bandyopadhyay A and Trivedi AK. BMP signaling-driven osteogenesis is critically dependent on Prdx-1 expression-mediated maintenance of chondrocyte prehypertrophy. *Free Radic Biol Med* 2018; 118: 1-12.
- [11] Yu C, Li L, Xie F, Guo S, Liu F, Dong N and Wang Y. LncRNA TUG1 sponges miR-204-5p to promote osteoblast differentiation through upregulating Runx2 in aortic valve calcification. *Cardiovasc Res* 2018; 1: 168-179.
- [12] Sun W, Zhao R, Yang Y, Wang H, Shao Y and Kong X. Comparative study of human aortic and mitral valve interstitial cell gene expression and cellular function. *Genomics* 2013; 6: 326-335.
- [13] Hjortnaes J, Shapero K, Goettsch C, Hutcheson JD, Keegan J, Kluijn J, Mayer JE, Bischoff J and Aikawa E. Valvular interstitial cells suppress calcification of valvular endothelial cells. *Atherosclerosis* 2015; 242: 251-260.
- [14] Azpiazu D, Gonzalo S, González-Parra E, Egido J and Villa-Bellosta R. Role of pyrophosphate in vascular calcification in chronic kidney disease. *Nefrologia* 2018; 3: 250-257.
- [15] Toita R, Otani K, Kawano T, Fujita S, Murata M and Kang JH. Protein kinase A (PKA) inhibition reduces human aortic smooth muscle cell calcification stimulated by inflammatory response and inorganic phosphate. *Life Sci* 2018; 209: 466-471.
- [16] Go AS, Mozaffarian D, Roger VL, Benjamin EJ, Berry JD, Borden WB, Bravata DM, Dai S, Ford ES, Fox CS, Franco S, Fullerton HJ, Gillespie C, Hailpern SM, Heit JA, Howard VJ, Huffman MD, Kissela BM, Kittner SJ, Lackland DT, Lichtman JH, Lisabeth LD, Magid D, Marcus GM, Marelli A, Matchar DB, McGuire DK, Mohler ER, Moy CS, Mussolino ME, Nichol G, Paynter NP, Schreiner PJ, Sorlie PD, Stein J, Turan TN, Virani SS, Wong ND, Woo D and Turner MB; American Heart Association Statistics Committee and Stroke Statistics Subcommittee. Executive summary: heart disease and stroke statistics—2013 update: a report from the American heart association. *Circulation* 2013; 127: 143-152.
- [17] Yutzey KE, Demer LL, Body SC, Huggins GS, Towler DA, Giachelli CM, Hofmann-Bowman MA, Mortlock DP, Rogers MB, Sadeghi MM and Aikawa E. Calcific aortic valve disease: a consensus summary from the alliance of investigators on calcific aortic valve disease. *Arterioscler Thromb Vasc Biol* 2014; 11: 2387-2393.
- [18] Rathana S, Yoganathan AP and O'Neill CW. The role of inorganic pyrophosphate in aortic valve calcification. *J Heart Valve Dis* 2014; 4: 387-394.
- [19] Liu Y, Zhang L, Ni Z, Qian J and Fang W. Calcium phosphate crystals from uremic serum promote osteogenic differentiation in human aortic smooth muscle cells. *Calcif Tissue Int* 2016; 5: 543-555.
- [20] Neven E, Opdebeeck B, De Maré A, Bashir-Dar R, Dams G, Marynissen R, Behets GJ, Verhulst A, Riser BL and D'Haese PC. Can intestinal phosphate binding or inhibition of hydroxyapatite growth in the vascular wall halt the progression of established aortic calcification in chronic kidney disease. *Calcif Tissue Int* 2016; 5: 525-534.
- [21] Yamada S, Tatsumoto N, Tokumoto M, Noguchi H, Ooboshi H, Kitazono T and Tsuruya K. Phosphate binders prevent phosphate-induced cellular senescence of vascular smooth muscle cells and vascular calcification in a modified, adenine-based uremic rat model. *Calcif Tissue Int* 2015; 4: 347-358.
- [22] Goto S, Rogers MA, Blaser MC, Higashi H, Lee LH, Schlotter F, Body SC, Aikawa M, Singh SA

- and Aikawa E. Standardization of human calcific aortic valve disease in vitro modeling reveals passage-dependent calcification. *Front Cardiovasc Med* 2019; 6: 49.
- [23] Ardeshiryajimi A, Golchin A, Khojasteh A and Bandehpour M. Increased osteogenic differentiation potential of MSCs cultured on nanofibrous structure through activation of Wnt/ β -catenin signalling by inorganic polyphosphate. *Artif Cells Nanomed Biotechnol* 2018; 46: S943-S949.
- [24] Li XF, Wang Y, Zheng DD, Xu HX, Wang T, Pan M, Shi JH and Zhu JH. M1 macrophages promote aortic valve calcification mediated by microRNA-214/TWIST1 pathway in valvular interstitial cells. *Am J Transl Res* 2016; 12: 5773-5783.
- [25] Zeng Q, Jin C, Ao L, Cleveland JC Jr, Song R, Xu D, Fullerton DA and Meng X. Cross-talk between the Toll-like receptor 4 and Notch1 pathways augments the inflammatory response in the interstitial cells of stenotic human aortic valves. *Circulation* 2012; Suppl 1: S222-230.
- [26] Kishimoto T, Akira S and Taga T. Interleukin-6 and its receptor: a paradigm for cytokines. *Science* 1992; 5082: 593-597.
- [27] El HD, Boulanger MC, Mahmut A, Bouchareb R, Laflamme MH, Fournier D, Pibarot P, Bosse Y and Mathieu P. P2Y2 receptor represses IL-6 expression by valve interstitial cells through Akt: implication for calcific aortic valve disease. *J Mol Cell Cardiol* 2014; 72: 146-156.
- [28] Yao Y, Bennett BJ, Wang X, Rosenfeld ME, Giachelli C, Lusis AJ and Boström KI. Inhibition of bone morphogenetic proteins protects against atherosclerosis and vascular calcification. *Circ Res* 2010; 4: 485-494.
- [29] Dhore CR, Cleutjens JP, Lutgens E, Cleutjens KB, Geusens PP, Kitslaar PJ, Tordoir JH, Spronk HM, Vermeer C and Daemen MJ. Differential expression of bone matrix regulatory proteins in human atherosclerotic plaques. *Arterioscler Thromb Vasc Biol* 2001; 12: 1998-2003.
- [30] Zebboudj AF, Shin V and Bostrom K. Matrix GLA protein and BMP-2 regulate osteoinduction in calcifying vascular cells. *J Cell Biochem* 2003; 4: 756-765.
- [31] Lucaciu O, Soritau O, Gheban D, Ciuca DR, Virtic O, Vulpoi A, Dirzu N, Campian R, Baciut G, Popa C, Simon S, Berce P, Baciut M and Crisan B. Dental follicle stem cells in bone regeneration on titanium implants. *BMC Biotechnol* 2015; 15: 114.
- [32] Derwall M, Malhotra R, Lai CS, Beppu Y, Aikawa E, Seehra JS, Zapol WM, Bloch KD and Yu PB. Inhibition of bone morphogenetic protein signaling reduces vascular calcification and atherosclerosis. *Arterioscler Thromb Vasc Biol* 2012; 3: 613-622.
- [33] Kaden JJ, Bickelhaupt S, Grobholz R, Vahl CF, Hagl S, Brueckmann M, Haase KK, Dempfle CE and Borggrefe M. Expression of bone sialoprotein and bone morphogenetic protein-2 in calcific aortic stenosis. *J Heart Valve Dis* 2004; 4: 560-566.
- [34] Byon CH, Javed A, Dai Q, Kappes JC, Clemens TL, Darley-Usmar VM, McDonald JM and Chen Y. Oxidative stress induces vascular calcification through modulation of the osteogenic transcription factor Runx2 by AKT signaling. *J Biol Chem* 2008; 22: 15319-15327.
- [35] Morrell NW, Bloch DB, ten Dijke P, Goumans MJ, Hata A, Smith J, Yu PB and Bloch KD. Targeting BMP signalling in cardiovascular disease and anaemia. *Nat Rev Cardiol* 2016; 2: 106-120.
- [36] Lee KS, Kim HJ, Li QL, Chi XZ, Ueta C, Komori T, Wozney JM, Kim EG, Choi JY, Ryoo HM and Bae SC. Runx2 is a common target of transforming growth factor beta1 and bone morphogenetic protein 2, and cooperation between Runx2 and Smad5 induces osteoblast-specific gene expression in the pluripotent mesenchymal precursor cell line C2C12. *Mol Cell Biol* 2000; 23: 8783-8792.
- [37] Matsubara T, Kida K, Yamaguchi A, Hata K, Ichida F, Meguro H, Aburatani H, Nishimura R and Yoneda T. BMP2 regulates Osterix through Msx2 and Runx2 during osteoblast differentiation. *J Biol Chem* 2008; 43: 29119-29125.
- [38] Chen Z, Wang X, Shao Y, Shi D, Chen T, Cui D and Jiang X. Synthetic osteogenic growth peptide promotes differentiation of human bone marrow mesenchymal stem cells to osteoblasts via RhoA/ROCK pathway. *Mol Cell Biochem* 2011; 1-2: 221-227.
- [39] Itzstein C, Coxon FP and Rogers MJ. The regulation of osteoclast function and bone resorption by small GTPases. *Small GTPases* 2011; 3: 117-130.
- [40] Asama H, Suzuki T, Kita E, Matsushashi N, Ichii O, Tai M, Ejiri Y and Ohira H. Nonalcoholic steatohepatitis after pancreatoduodenectomy with rapid progression of hepatic fibrosis: a case report. *Nihon Shokakibyō Gakkai Zasshi* 2015; 5: 905-913.
- [41] Tai BC, Du C, Gao S, Wan AC and Ying JY. The use of a polyelectrolyte fibrous scaffold to deliver differentiated hMSCs to the liver. *Biomaterials* 2010; 1: 48-57.
- [42] Gu X and Masters KS. Role of the Rho pathway in regulating valvular interstitial cell phenotype and nodule formation. *Am J Physiol Heart Circ Physiol* 2011; 2: H448-458.
- [43] Farrar EJ, Pramil V, Richards JM, Mosher CZ and Butcher JT. Valve interstitial cell tensional homeostasis directs calcification and extracel-

Stimulated osteogenesis of VICs via RhoA/ROCK-1 and BMP-2/Smad signaling

- ular matrix remodeling processes via RhoA signaling. *Biomaterials* 2016; 105: 25-37.
- [44] Wang YK, Yu X, Cohen DM, Wozniak MA, Yang MT, Gao L, Eyckmans J and Chen CS. Bone morphogenetic protein-2-induced signaling and osteogenesis is regulated by cell shape, RhoA/ROCK, and cytoskeletal tension. *Stem Cells Dev* 2012; 7: 1176-1186.
- [45] Zhu YT, Li F, Han B, Tighe S, Zhang S, Chen SY, Liu X and Tseng SC. Activation of RhoA-ROCK-BMP signaling reprograms adult human corneal endothelial cells. *J Cell Biol* 2014; 6: 799-811.
- [46] Sung DC, Bowen CJ, Vaidya KA, Zhou J, Chapurin N, Recknagel A, Zhou B, Chen J, Kotlikoff M and Butcher JT. Cadherin-11 overexpression induces extracellular matrix remodeling and calcification in mature aortic valves. *Arterioscler Thromb Vasc Biol* 2016; 8: 1627-1637.
- [47] Fedak PW, Verma S, David TE, Leask RL, Weisel RD and Butany J. Clinical and pathophysiological implications of a bicuspid aortic valve. *Circulation* 2002; 8: 900-904.
- [48] Gotoh T, Kuroda T, Yamasawa M, Nishinaga M, Mitsuhashi T, Seino Y, Nagoh N, Kayaba K, Yamada S and Matsuo H. Correlation between lipoprotein(a) and aortic valve sclerosis assessed by echocardiography (the JMS cardiac echo and cohort study). *Am J Cardiol* 1995; 12: 928-932.
- [49] Helske S, Kupari M, Lindstedt KA and Kovanen PT. Aortic valve stenosis: an active atheroinflammatory process. *Curr Opin Lipidol* 2007; 5: 483-491.
- [50] Wang B, Li F, Zhang C, Wei G, Liao P and Dong N. High-mobility group box-1 protein induces osteogenic phenotype changes in aortic valve interstitial cells. *J Thorac Cardiovasc Surg* 2016; 1: 255-262.
- [51] Wang Y, Xiao X, Zhou T, Han D and Dong N. Novel mechanisms for osteogenic differentiation of human aortic valve interstitial cells. *J Thorac Cardiovasc Surg* 2020; 159: 1742-1753, e7.
- [52] Liu AC, Joag VR and Gotlieb AI. The emerging role of valve interstitial cell phenotypes in regulating heart valve pathobiology. *Am J Pathol* 2007; 5: 1407-1418.